Measuring the Dispersion Forces Near the van der Waals–Casimir Transition

V.B. Svetovoy,[1,*] A.V. Postnikov,[2] I.V. Uvarov,[2] F.I. Stepanov,[3] and G. Palasantzas[4]

[1] *A. N. Frumkin Institute of Physical Chemistry and Electrochemistry, Russian Academy of Sciencies, Leninsky prospect 31 bld. 4, Moscow 119071, Russia*

[2] *Valiev Institute of Physics and Technology, Yaroslavl Branch, Russian Academy of Sciences, Universitetskaya 21, Yaroslavl 150007, Russia*

[3] *Ishlinsky Institute for Problems in Mechanics, Russian Academy of Sciences, prospect Vernadskogo, 101-1, Moscow 119526, Russia*

[4] *Zernike Institute for Advanced Materials, University of Groningen – Nijenborgh 4, Groningen, AG 9747, Netherlands*

(Received 24 April 2020; accepted 5 June 2020; published 23 June 2020)

Forces induced by quantum fluctuations of the electromagnetic field control adhesion phenomena between rough solids when the bodies are separated by distances of approximately 10 nm. However, this distance range remains largely unexplored experimentally in contrast with the shorter (van der Waals forces) or the longer (Casimir forces) separations. The reason for this is the pull-in instability of the systems with the elastic suspension that poses a formidable limitation. In this paper we propose a genuine experimental configuration that does not suffer from the short distance instability. The method is based on the adhered cantilever, whose shape is sensitive to the forces acting near the adhered end. The general principle of the method, its possible realization, and feasibility are extensively discussed. The dimensions of the cantilever are determined by the maximum sensitivity to the forces. If the adhesion is defined by strong capillary or chemical interactions, the method loses its sensitivity. Special discussion is presented for the determination of the minimum distance between the rough solids upon contact, and for the compensation of the residual electrostatic contribution. The proposed method can be applied to any kind of solids (metals, semiconductors, or dielectrics) and to any intervening medium (gas or liquid).

DOI: 10.1103/PhysRevApplied.13.064057

I. INTRODUCTION

The interaction between three-dimensional bodies induced by quantum fluctuations of the electromagnetic field becomes important at short separations, less than 100 nm. This interaction results in attractive dispersion forces (DFs) [1,2], which include van der Waals (vdW) and Casimir forces. Lifshitz and coauthors [3,4] demonstrated that both forces are the asymptotics of one and the same force at long (Casimir) and at short (vdW) distances. DFs have been actively investigated for the last 20 years [5,6]. In a series of critical experiments [7–11] the forces were measured at distances greater than or similar to 100 nm with a high precision of approximately 1%. The results agree with the prediction of the Lifshitz theory [3,4] that accounts for finite temperature and dielectric response of the interacting bodies. The latter dependence was checked in a number of experiments performed for different materials [12–16]. The contribution of thermal fluctuations to the force is not important at distances $d \lesssim 100$ nm.

All the modern experiments are performed with the use of microelectromechanical systems (MEMSs), which are characterized by a small separation between elements and large areas of these elements. Under these conditions (small distance and large area), DFs manifest most distinctly. Irreversible adhesion (stiction) of moving MEMS elements induced by DFs results in failure of MEMS devices [17–19]. During operation of the device, stiction can occur owing to the pull-in instability and at the fabrication stage, it can be induced by capillary forces. The stiction problem seriously restricts applications of MEMSs. It is worth noting that strong adhesion by chemical interactions or by capillary forces can be excluded by special preparation of the surfaces, but a relatively weak adhesion owing to DFs cannot be excluded in principle. The latter adhesion is responsible for many natural phenomena (for example, a firm grip of geckos on walls and ceilings [20]) and for many artificial processes (for example, stiction of a polymeric film to surfaces [21]). This adhesion forms an entire class of physical phenomena, which often appear in the surrounding world. DFs produce not only a negative effect on MEMSs but can be used to control the devices.

*v.svetovoy@utwente.nl

Actuation of MEMS devices with the vdW-Casimir forces is a dynamically developing field [22–32].

When two solids come into contact, they are still separated by the average distance $d \sim 10$ nm owing to the finite roughness of contacting bodies. This distance range corresponds to the transition between vdW and Casimir forces, which physically means the transition between the retarded and unretarded interaction. This range was studied much less than the range $d \gtrsim 100$ nm, although DFs at shorter distances play a more important role. Poor knowledge of the forces in the transition region is related to the same pull-in instability that leads to stiction of the MEMS elements. In the experiments the force is balanced by a spring of known stiffness k, as shown schematically in Fig. 1. A principal disadvantage of such a system is the loss of stability at short separations. In some experiments the spring is a cantilever of the atomic force microscope (AFM) [8,13,15,16]. In other experiments this role belongs to a torsional rod [9–11,14] or to a string [7]. In all but one [33] of the experiments the force was measured between a sphere and plate to avoid the parallelism problem. Because of the strong surface charging of dielectrics, the force was measured between well-conductive materials or doped semiconductors [7–15].

In practice, the shortest jump-to-contact distance was 12 nm for the AFM experiment with a very stiff cantilever [34]. It is much smaller than the minimal distance for high precision experiments (from 40 nm [15] to 150 nm [11]). The surface force apparatus [35] that uses much stiffer springs is more stable, but even in this case the shortest distance (in a vacuum) was about 8.5 nm [36]. Only two measurements exist at these short separations between good conductors (Au-Au) [34,36], while a similar short-range measurement was also performed between a very flat nitrogen doped SiC and low roughness Au surfaces [37]. Precision of the short-distance experiments is low because the absolute uncertainty in the separation $\delta d \sim 1$ nm gives a large relative error in the force measurement, approximately $\alpha(\Delta d/d)$, where $2 < \alpha < 3$ for the sphere-plate configuration. Because of the pull-in instability, the data in the short-distance range $d \sim 10$ nm are sparse and have poor precision, although in this range the role of the DFs is crucial for many physical phenomena.

To theoretically predict the force at short distances is as difficult as to measure it. The problem occurs due to the nonadditivity of DFs. "In condensed bodies (in contrast with gases) the atoms in the neighbourhood cause an essential change in the properties of the electronic shells, and the presence of a medium between the interacting atoms affects the electromagnetic field fluctuations through which the interaction is established" [4]. While the root-mean-square (rms) roughness is small in comparison with the distance between the bodies, the roughness contribution can be evaluated as a perturbative effect [38,39]. However, when the roughness amplitude is comparable with the separation gap, there is no reliable way to predict the force (see Ref. [40] on the nonadditive roughness effects).

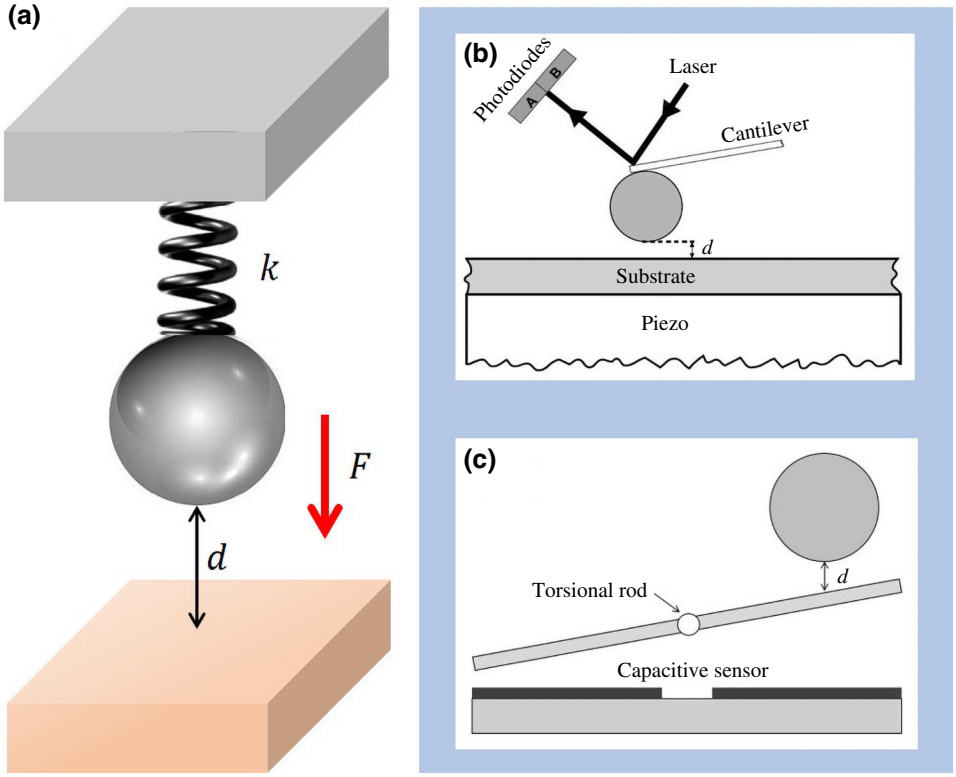

FIG. 1. (a) Schematic view for the standard way to measure the force between a sphere and a plate. The force F is balanced by a spring of stiffness k. (b) AFM realization [8]. (c) Torsional rod realization [9].

The nonperturbative roughness contribution was observed [41] as a strong deviation from the expected power-law scaling for rough bodies close to contact. Qualitatively this effect was observed even earlier [27]. An approach to deal theoretically with the roughness problem was proposed by Broer *et al.* [42] and then developed in more detail [43]. The idea of the method is based on a so-called "grass and trees" model. High peaks (trees), which define the minimum distance between the bodies (distance upon contact), are rare and the average distance between them is large. For this reason, their contribution can be calculated additively. On the other hand, the asperities with heights close to the rms roughness (grass) can be calculated using perturbation theory. This approach successfully reproduced the experimental results for very rough gold surfaces [43], but the experimental precision was not sufficient to check the model for smoother surfaces, and discriminate between the additive and nonadditive contributions. Moreover, roughness of deposited gold films is described by extreme value statistics [44], and it is not clear if one can apply the model for other statistics as well.

In this paper we propose a method to measure the dispersion forces between rough solids close to contact. The method is based on the adhered cantilever and does not suffer from the loss of stability at short separations. It also allows us to test models for evaluation of the roughness contribution into dispersion forces at distances comparable with the roughness amplitude.

II. METHOD OF THE ADHERED CANTILEVER

The stiction problem in MEMSs has been analysed experimentally and theoretically [18,19] for a model system that is the adhered cantilever shown in Fig. 2. One end of a rectangular flexible beam is firmly fixed at a height h above a substrate. If the beam is long enough, the other end will stick to the substrate after the last step of the fabrication process (drying). It was demonstrated [45,46] that the adhesion energy per unit area Γ is related to the unadhered part of the cantilever of length s and, using this relation, an accurate method to determine Γ has been proposed [47]. Simultaneous influence of the adhesion and electrostatic forces on the shape of the cantilever has also been addressed [48].

A. Idea of the method

In the adhered area the attractive forces (dispersion, electrostatic, capillary, chemical) are equilibrated by the repulsion owing to elastic deformation of roughness asperities of the solids in contact. Outside of the adhered area, but close to it (see the highlighted area in Fig. 2), the vdW-Casimir force between the beam and substrate is equilibrated by the elastic force owing to bending of the cantilever. This force has to influence the shape of the cantilever. Moreover, this influence has to be appreciable far away from the adhered end owing to the boundary condition $du/dx = 0$ at $x = 0$, where $u(x)$ is the shape of the cantilever, as shown in Fig. 2. Since the adhered cantilever is always in a stable state, we can measure the forces acting near the adhered end without the distance restrictions. This can be achieved by analysing the shape of the cantilever. This is the main point of the proposed method, but to see its feasibility we have to consider the problem in more detail.

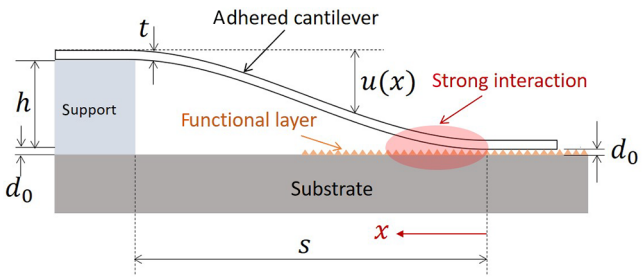

FIG. 2. Adhered cantilever. The main parameters and the choice of coordinate system are shown. The domain, where the dispersion force between the cantilever and substrate is strong, is highlighted. The minimum distance d_0 between the cantilever and substrate is established by roughness of the solids.

An attempt to numerically calculate the change in shape owing to vdW forces was carried out by Knapp and de Boer [48]. They concluded that the effect is negligible; however, their calculations covered an unfavorable parameter range. More detailed analytic and numerical analyses [49] demonstrated existence of a parameter range in which the force influences the shape of the cantilever on a measurable level.

B. Shape of the cantilever

If we completely neglect external forces acting on the unadhered part, the cantilever has the classic shape

$$u_0(x) = h(1 - 3\xi^2 + 2\xi^3), \qquad \xi = x/h, \tag{1}$$

which is defined by the balance of the adhesion and elastic forces [48]. In reality, outside of the adhered area the cantilever interacts with the substrate via the gas (or liquid) gap owing to the DFs and the residual electrostatic forces. The latter can appear as a contact potential difference or as surface charges owing to trapped charge in the dielectrics. The electrostatic force can be compensated as discussed below (see Sec. III F) so that in the external force we include only the DF. Solving the elasticity theory equations we can find the correction to the classical shape owing to the external force [49]. This correction is shown in Fig. 3. For simplicity, the DF per unit area is given in a form that is well justified in the restricted range of distances [50]

$$P(d) = P_0(d/d_0)^{-\alpha}, \tag{2}$$

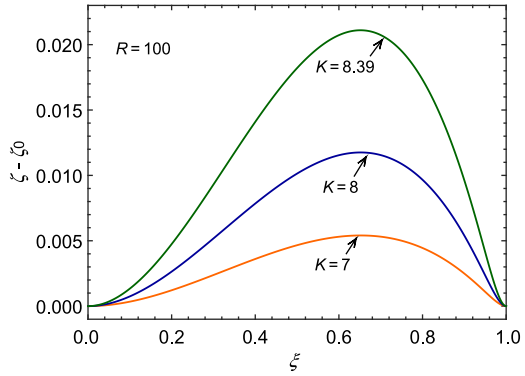

FIG. 3. Normalized deviation of the shape of the cantilever $\zeta = u(x)/h$ from the classic shape $\zeta_0 = u_0(x)/h$ as a function of the lateral coordinate $\xi = x/s$. The results are presented for a few values of the parameter K, which is proportional to the dispersion pressure P_0 at the minimum separation d_0. The data for the figure is taken from Ref. [49].

where, for the plate-plate interaction, the exponent $\alpha = 3$ corresponds to a pure vdW force and $\alpha = 4$ corresponds to a pure Casimir force. The actual situation can be described by an intermediate parameter $3 < \alpha < 4$. The parameter P_0 has the meaning of the dispersion pressure at the minimum distance d_0. An important parameter characterising the problem is $R = h/d_0 \gg 1$, which is always large for any practical situation.

As can be seen from Fig. 3, the deviation $\Delta u = u(x) - u_0(x)$ is maximum at $x = s/3$, which is far away from the adhered end. The width of the domain, where the force is strong, is estimated as the lateral size of the region where the vertical distance between the beam and substrate is $d < 2d_0$ that corresponds to a force reduction of roughly one order of magnitude. It gives a width of approximately $s\sqrt{d_0/h} \ll s/3$. This property is especially convenient for the force measurement. The relative value of Δu at maximum reaches a few percents and strongly depends on the parameter K that is defined as the ratio of the dispersion pressure at the smallest distance d_0 to an elastic pressure P_s:

$$K = (P_0/P_s)^{1/4}, \qquad P_s = Et^3h/12s^4. \tag{3}$$

Here E is Young's modulus of the beam material and t is the thickness of the cantilever. When the parameter K reaches a critical value K_c, the deviation Δu reaches its maximum and scales as $\Delta u \sim \sqrt{d_0 h}$. The value of $K > K_c$ cannot be reached because in response to a too large force the unadhered length s will be reduced, resulting in K smaller than the critical value. Therefore, the experiment has to be designed to keep the value of K as close as possible to K_c, where the sensitivity to the DF acting near the adhered end is largest.

C. Work done by the DF

To determine the force, we can measure the unadhered length s and the maximum deviation from the classic shape $\Delta u_{\max} = \Delta u(s/3)$. From these two values, it is possible to find the force at the minimum distance P_0 and the adhesion energy Γ. Because bending of the cantilever depends on the force in an integral way, the deviation Δu is defined only by the force at d_0. The adhesion energy Γ depends weakly on the external force and we can use the classic relation [47]

$$\Gamma \approx \frac{3Et^3h^2}{2s^4}. \tag{4}$$

The relative correction to this relation owing to the DF [49] scales as $R^{-3/2}$.

Combining Eqs. (3) and (4) we can present the parameter K via Γ and P_0 as

$$K^4 = 18R\left(\frac{d_0P_0}{\Gamma}\right). \tag{5}$$

It follows from (2) that the work done against the DF to put the cantilever at the position $d = d_0$ is given by

$$W = d_0P_0/(\alpha - 1). \tag{6}$$

Therefore, K^4 is proportional to the ratio of W to the adhesion energy. In general, there are a number of sources contributing to the adhesion energy, but, if the adhesion is defined only by the dispersion interaction, $\Gamma = W$ takes the smallest value, resulting in the largest K (highest sensitivity). For this case, we find that $K = 2.59R^{1/4}$, while the critical value determined in Ref. [49] is $K_c = 2.65R^{1/4}$ (both values are presented for $\alpha = 3.5$). We see that the highest sensitivity to the force is realized for the weakest adhesion, when K is close to the critical value. The possibility to reach the weakest adhesion was demonstrated experimentally [27]. On the other hand, for strong adhesion $\Gamma \gg W$, the shape of the cantilever approaches the classic shape and the method of the adhered cantilever will not be sensitive to the DF anymore.

D. Advantages and disadvantages of the method

The method of the adhered cantilever has the following advantages over the method of elastic suspension.

(i) No pull-in instability at short distances. This is the most important property that allows measurement of the forces at short distances, which are difficult or impossible to examine using the elastic suspension method.

(ii) The force and the adhesion energy are measured simultaneously. This property allows separation of the dispersion contribution to the adhesion energy.

(iii) The force is measured between practically parallel plates. No parallelism problem appears in contrast with the elastic suspension method.

(iv) No restriction on the used materials. The materials can be metals, semiconductors, or dielectrics and any combination of two different materials. Because of trapped charges in the dielectrics, measurement of the DF is problematic for the elastic suspension.

(v) The force can be measured in a gas or liquid environment with comparable precision. The method of elastic suspension suffers from a significant loss of precision if the force is measured in a liquid.

However, there are disadvantages of the adhered cantilever method.

(a) The force can be measured at only one specific distance d_0 corresponding to the minimum distance between solids. This distance can be changed only by changing the roughness of the interacting solids.

(b) The method is sensitive to accidental nanoparticles in the adhered area, although the presence of these particles can be easily recognized. This demands assembling the measuring chips in very clean conditions.

III. CONFIGURATION OF THE EXPERIMENT

A. Optimal dimensions

Since adhered cantilevers were originally used as model systems to analyze the stiction problem in MEMSs, the cantilevers dimensions were typical for micromechanics [18,27,48]: width $w = 20$–30 μm, thickness $t = 2$–3 μm, support height $h = 2$ μm, and total length $L = 1000$–1500 μm. For $d_0 = 10$ nm and $h = 2$ μm, the maximum deviation from the classical shape is estimated as $\Delta u_{\max} \approx 34$ nm [49] [see Eq. (3) below]. This value is measurable by any interferometric method, but to increase precision and widen the available range of parameters, it is preferable to have larger deviations.

Larger deviations can be achieved by increasing the support height h to a value of 10–20 μm when $\Delta u_{\max} = 77$–108 nm. Moreover, thin cantilevers made of polysilicon by microfabrication can deviate from ideal behavior owing to a nonzero take-off angle at the fixed end, finite torsional compliance, and initial nonzero curvature of the unadhered cantilever [51]. This nonideality can also influence the shape of the cantilever, introducing significant uncertainties. To significantly reduce these effects, we propose to fabricate the cantilevers from a single crystal silicon. This is possible by using silicon-on-insulator (SOI) wafers, for which the thickness of the top layer Si above SiO_2 is $t = 10$–15 μm. For an estimate, using $t = h = 10$ μm and a typical value of the adhesion energy induced by the dispersion forces $\Gamma = 10$ μJ/m^2, we find from Eq. (4) that the unadhered length of the cantilever $s \approx 7$ mm. From this estimate we can conclude that the total length of the cantilever has to be about $L = 10$ mm. A convenient width for these long cantilevers is $w = 1$ mm. In comparison with microcantilevers suggested by MEMSs, these single crystal minibeams are sufficiently soft but more convenient for handling. Moreover, owing to a large adhered area, the adhesion energy Γ is a well-defined parameter with a small place-to-place variation.

B. Chip design

The chips for measurements will be assembled from two silicon wafers, as shown in Fig. 4. The top layer is a polished Si with a thickness t that is separated from the base Si layer by a thin silicon dioxide layer. The cantilevers are fabricated in the top layer and the base layer under the cantilevers is etched away by plasma etching using SiO_2 as a stop layer. The cantilevers are released by wet etching of SiO_2 in hydrofluoric acid. The second wafer is an ordinary Si wafer covered with the negative SU-8 photoresist of thickness h, which is used as the support for the cantilevers. Both wafers are bonded together as shown in Fig. 4(b). The front sides of the wafers are facing each other and the cantilevers are deflected away from the landing pads owing to gravity (the free end is deflected about 40 μm). Alignment is easy owing to rather large lateral sizes of the beams. Rotating the pile topside up as shown in Fig. 4(a) will result in the adhesion of cantilevers induced by gravity.

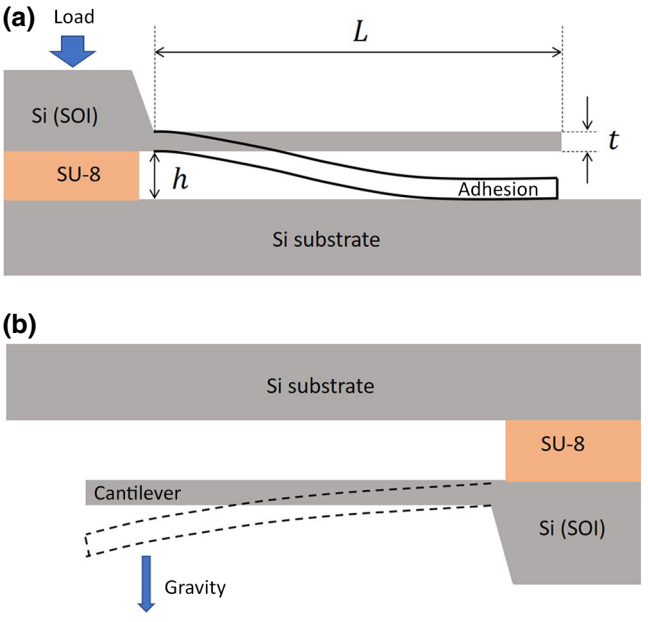

FIG. 4. (a) Measuring unit. The chip is assembled from a SOI wafer containing the single crystal Si cantilever and a common Si wafer separated by a layer of SU-8. (b) Upside down assembling of the wafers to prevent initial adhesion.

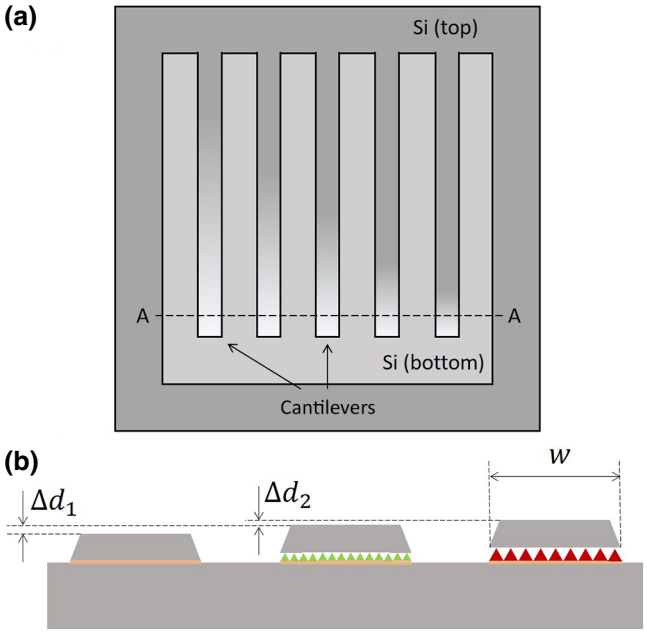

FIG. 5. (a) Top view of the chip. Each cantilever can have a different unadhered length (shown in gray scale). Areas covered by the top and bottom wafers are indicated. (b) Cross section along the AA line (adhered ends). The height difference is due to different functional layers at the landing pads.

One wafer of 100 mm in diameter will contain 12 chips with a size of 18 × 18 mm. Each chip includes five identical beams, as shown in Fig. 5, but the ends of each beam and the corresponding landing pad can be covered with different functional layers. Because of the difference between the adhesion energies of the beam and the landing pad, the unadhered length s for each cantilever in the series will vary. As functional layers, we plan to use different metals, semiconductors, and dielectrics, and different kinds of nanoparticles deposited on Si wafers. There are many possibilities to change the roughness of the functional layer even for the same functional material. This leads the way to varying the minimum distance d_0 and, therefore, to measuring the forces at different distances.

C. Characterization

Before assembling the top and bottom wafers, the ends of the cantilevers and the corresponding landing pads can be characterized for roughness using an AFM. This possibility is an important advantage of the chip design. Since the minimum distance between the solids d_0 is defined by the highest asperities, we have to know not only the roughness distribution around the most probable height, but also the tail of the distribution for the highest asperities. The latter is a nontrivial problem because to collect reliable statistics for rare events (high peaks), we have to analyze as large an area as possible. Nevertheless, it is feasible, as was demonstrated in Ref. [44] where Au films were investigated using AFM scans with a size of 20 × 20 μm^2 and with a resolution of 4096 × 4096 pixels. It was found that high peaks on gold films are well described by extreme value statistics rather than by the tail of the normal distribution. For the adhered cantilever experiment, there is room to improve the data collection and transformation.

Furthermore, it is important to know with the best possible precision the minimum distance between the solids d_0. It is essential because uncertainties in d_0 define the relative error in the force measurement. This can be achieved by scanning along the line AA shown in Fig. 5(b) with the laser beam of an interferometer. Because the total thickness to measure is about 10 μm but the target precision is 1 nm, we need the interferometer with a high dynamic range. For this purpose, we can use a homodyne Michelson interferometer with quadrature signals [52,53]. Feasibility of this method was checked with a homemade interferometer [54] of this kind (see Sec. III D). The same interferometer can be used for determining eigenfrequencies and quality factors of the cantilevers, recording free oscillations in air and/or in vacuum excited with a piezo. These values provide auxiliary information on the cantilevers.

Among five cantilevers in the chip one can be used to calibrate the distance d_0. This cantilever and the corresponding landing pad have no functional layers. Therefore, in the adhered area two very smooth (rms roughness 0.2–0.3 nm) Si surfaces meet. The average separation distance between these surfaces can be reliably predicted using proximity force approximation and detailed information on the surface roughness. The values of d_0 for all the other cantilevers on the chip can be determined from the interferometric measurements, as shown in Fig. 5(b).

An additional important characteristic of the cantilever is the uniformity of the thickness t. For SOI wafers, the producers guarantee the thickness of the top working layer at the level of ±0.5 μm over the entire wafer scale. This is much larger than the deviations from the classical shape, which we will measure. Therefore, the thickness of the cantilevers has to be carefully characterized over their length. This can be achieved using the wavelength $\lambda =$ 1.15 μm (HeNe laser), for which silicon is transparent. Interference of the light reflected from the top and from the bottom sides of the cantilever carries information on the thickness t at a given position of the laser beam.

D. Shape of the cantilever

The cantilever beam has the classical shape (1) if the adhesion energy Γ is large in comparison with the work W (6) done by the DF. The classic shape can be tested for strong adhesion induced, for example, by capillary interaction. To this end, hydrophilic cantilevers can be tested in a humid atmosphere. To keep the unadhered length s in the same range, we can increase the thickness h of the

separating SU-8 layer for some chips. The effects from nonzero take-off angle and finite torsional compliance [51] have to be small because the cantilevers are made from a single piece of crystalline silicon, but even small effects can be characterized with the interferometer and taken into account in the analysis. The same can be done with the initial curvature of the cantilever that is *a priori* not negligible.

The shape of an adhered beam can be measured by scanning along the cantilever with the laser beam of the interferometer. The quadrature signal interferometer is able to measure the change in the optical path with a precision of 1 nm in a wide dynamic range. The instrument has been used previously [54] to observe the movement of a flexible membrane driven by the electrochemical process. In Fig. 6 we show the data for the deflection of the membrane with time and the best fit for this nearly linear process. The difference between the data and the fit is shown in the inset. We can see that the rms noise stays within 1.2 nm, while the membrane deflects from 0 to 4.7 μm. This corresponds to a dynamic range of the interferometer of about 70 dB, but it can be increased further to 80 dB. This is because a small deflecting membrane is less convenient for observation than a flat cantilever that bends on a very small angle. This example demonstrates the feasibility of measuring the bending of the cantilever up to 10 μm with a precision of 1 nm.

From the scan of a specific cantilever we can determine the unadhered length s. Comparing the scan with the expected classic shape corrected to the initial nonzero

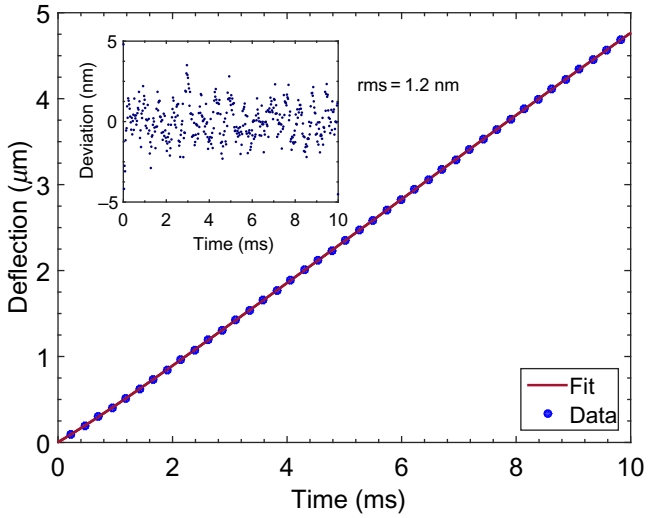

FIG. 6. Deflection of the actuator membrane [54] with time measured by the quadrature signal interferometer as a function of time. The best fit of the data is shown by the solid line. Only 10% of the data are shown. Deviation between the data (all points) and the fit is shown in the inset. The rms deviation is only 1.2 nm, while the total deflection is 4.7 μm. This figure is original, but it uses data from [54].

curvature and nonhomogeneous thickness, we find the maximum deviation from the classic shape at $x = s/3$. From the theory, this deviation is expected as [49]

$$\Delta u_{\max} \approx \left(\frac{2}{3}\right)^{7/2} \sqrt{d_0 h}\,\frac{d_0 P_0}{\Gamma(\alpha-1)}. \tag{7}$$

We see from this relation that the largest deviation is possible for the smallest Γ. The adhesion energy is the smallest for the case when it is defined completely by the dispersion forces $\Gamma = W$. Using Eq. (6), we find that the last factor is equal to 1. The method of adhered cantilever is favorable while $\Gamma \sim W$, but in the limit $\Gamma \gg W$ when strong adhesion forces dominate (for example, capillary) the condition for determining P_0 becomes unfavorable.

Let us estimate the expected values of W for Si-Si and Au-Au interactions at the distance $d_0 = 10$ nm. Assuming a pure vdW interaction $\alpha = 3$ (true only as a rough estimate), we have $W = A_H/12\pi d_0^2$, where A_H is the Hamaker constant for interacting materials. For Si-Si, this constant is $A_H = 2.6 \times 10^{-19}$ J [55] and, for Au-Au, it is $A_H = 4.5 \times 10^{-19}$ J [56]. Then, for the interaction energy between ideally flat surfaces, we find that $W = 69$ μJ/m^2 for Si-Si and $W = 119$ μJ/m^2 for Au-Au interactions. The unadhered length s increases with the thickness of cantilever t, while this length decreases with increasing adhesion energy. Thus, we can always choose a proper cantilever thickness t (or support height h) to work in the desired range of W.

From Eq. (7), the dispersion pressure P_0 at the minimum distance is expressed via the directly measurable parameters s, $\Delta u_{\max}$, and d_0. Defining uncertainties for each of the parameters by δ, we can express the relative error in the dispersion pressure as

$$\frac{\delta P_0}{P_0} = \left[\left(\frac{4\delta s}{s}\right)^2 + \left(\frac{\delta u}{\Delta u_{\max}}\right)^2 + \left(\frac{3\delta d_0}{2d_0}\right)^2\right]^{1/2}. \tag{8}$$

The relative uncertainty in the unadhered length s is estimated as 1%. The shape of the cantilever can be measured with a precision of $\delta u = 1$ nm. If the adhesion energy $\Gamma \sim W$ then the relative error in the shape is about 2%. The error in d_0 is the most important. It is defined by the precision with which we can measure the difference in the heights of the functional layers, which is $\delta d_0 = 1$ nm. This is a typical value realized for all the Casimir force experiments [8–15]. Since in our case d_0 is rather small, the relative error in the pressure owing to d_0 is estimated as 15%. We stress that, using the elastic suspension method, the same error in the pressure would be $\alpha\delta d_0/d_0$, which is more than twice as large ($\alpha > 3$). This occurs because the adhered cantilever method is sensitive to the integral effect of the force, but not directly to the force at a given distance.

E. Alternative determination of d_0

The force measured even with a poor precision at such short distances is of considerable interest. However, we propose a way to reduce δd_0 that is based on a large nominal area of contact for our cantilevers. For this purpose, we can combine the detailed roughness statistics of the contacting bodies with the prediction based on contact mechanics. The basis for this approach was proposed [34] and developed earlier [44], but only for a negligible load. Finite adhesion energy provides a significant load on high asperities, which come into contact with the opposing solid. These asperities are deformed elastically and possibly plastically, and their number can be determined from roughness statistics.

A rough plate is described as a set of asperities with a random height and with a lateral size that is given by the correlation length determined from the roughness topography. The height distribution is determined from the roughness analyzed over as large an area as possible. A large area is needed to collect reliable statistics of rare events, namely high asperities. These statistics can differ significantly from the normal distribution, as was demonstrated for deposited gold films [44]. It is important that the number of high asperities, which can be in contact with the opposing surface, depends on the analyzed area. In Fig. 7 we show the height of the highest asperity (equivalent to d_0 in the limit of zero load) as a function of the area size $\mathcal{L}$. We can see that this height increases with the size $\mathcal{L}$ and has a significant rms deviation owing to place-to-place variation of the highest peak. It has to be stressed that the rms deviation of d_0 decreases with the size $\mathcal{L}$. For a nominal adhered area of approximately 1 mm^2, which will be used in the proposed experiment, we expect a variation of d_0 considerably smaller than 1 nm.

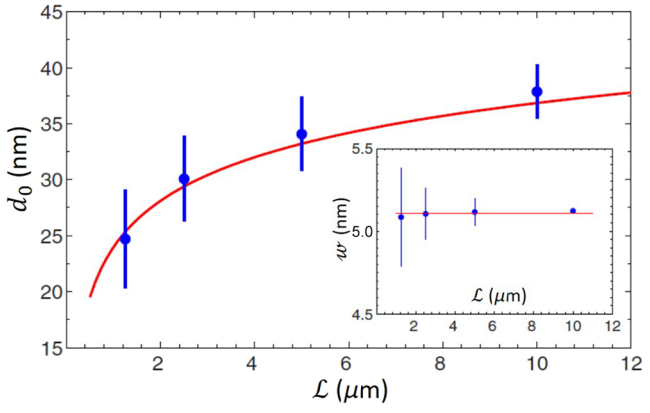

FIG. 7. Minimum distance d_0 between two plates allowed by their roughness at zero load. This distance depends on the analyzed area size $\mathcal{L}$ and varies from place to place (blue dots with error bars). The data are taken from AFM megascans of two gold films. The red curve is a theoretical prediction. The inset shows that the rms roughness does not depend on the size $\mathcal{L}$. The data for the figure is taken from Ref. [44].

The adhesion energy, which is extracted from the unadhered length of the cantilever, has to be equal to the free energy of N elastically deformed asperities of height d_0 and elastic modulus E. All peaks that are higher than d_0 are deformed plastically and their height is reduced to d_0. The number N of asperities with height $z > d_0$ within the area $\mathcal{L} \times \mathcal{L}$ is defined as $N = (\mathcal{L}^2/l_c^2)[1 - \mathcal{P}(d_0)]$ [44], where l_c is the correlation length and $\mathcal{P}(z)$ is the cumulative distribution of the asperity heights. The relative elastic deformation of these N asperities is determined from the balance of the elastic and adhesion energies. The same relative deformation defines the pressure acting on each asperity. In the simplest approach, when a peak is approximated by a bar with the cross-section area l_c^2, this pressure p is expressed as

$$p = \sqrt{(2\Gamma E/d_0)[1 - \mathcal{P}(d_0)]}. \tag{9}$$

It has to be equal to the plastic yield strength to prevent further deformation of the asperities. Equation (9) can be considered as the equation for the minimum distance d_0. Even this simplified model predicts reasonable values of d_0. For example, using the cumulative probability for 800 nm thick gold film (see Refs. [43,44]) and the adhesion energy induced by the dispersion interaction, we find from (9) that $d_0 = 33.7$ nm, while the value determined from the electrostatic calibration [41] for this film is $d_0 = 34.5 \pm 1.7$ nm.

This simple approach can be elaborated in detail. Realistic stress-strain curves can be used for each material; asperities can be modeled by hills of conical shape with rounded tips. Our aim is to reduce the error for determining d_0 to a value of $\delta d_0 \cong 0.2$–0.3 nm that is given by the roughness of Si wafers. In this case the dispersion force at $d_0 = 10$ nm can be determined with a relative precision of 5%. Prediction of d_0 based on the roughness topography and contact mechanics can be checked using the interferometric method for rather rough films. If the roughness is high, $\delta d_0 \sim 1$ nm determined interferometrically will be much smaller than d_0. Therefore, we can compare the prediction based on the topography with the interferometric measurement.

F. Compensation of electrostatic contribution

The residual electrostatic force is the most important background force that has to be compensated in all experiments measuring the Casimir force. This residual force appears because of a finite contact potential difference even between identical metals owing to a difference in wiring. The potential difference can be as high as a few hundred millivolts [7,10] and is reduced to a few tens of millivolts in the best cases [11]. The charges trapped in dielectrics

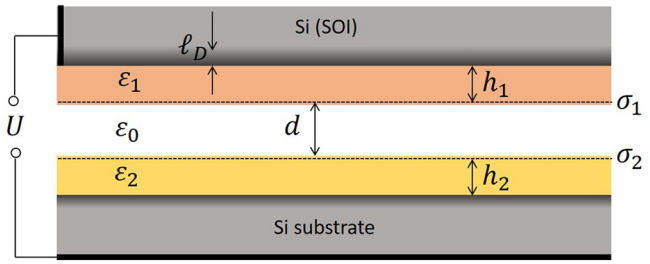

FIG. 8. Formation of the electrostatic pressure between solids approaching the contact. The Debye layer in Si is shown in gray scale. The dashed lines show the layers of surface charges with densities $\sigma_{1,2}$. An external potential difference U is applied between the Si wafers.

make it impossible to measure the Casimir force involving dielectric materials. Doping of dielectrics is used as a way to resolve the problem [37]. At short separations the electrostatic effect is less severe because the DF is much stronger, but compensation of the electrostatic force has to be done in this case too.

For the chip discussed in Sec. III B, we can make the electrical contacts to the layer with cantilevers and to the bottom of the chip. Silicon has a finite conductivity owing to doping and is characterized by a 13 nm thick Debye layer l_D for a carrier concentration of 10^{17} cm^{-3}. If the functional layers on the cantilever and landing pad are both dielectric, they can be charged with surface densities σ_1 and σ_2, respectively, as shown in Fig. 8. Neglecting the Debye layers in Si for simplicity, the electric field in the gap d is given by

$$E = -\frac{U + (4\pi\sigma_1/\varepsilon_1)h_1 - (4\pi\sigma_2/\varepsilon_2)h_2}{d + (\varepsilon_0/\varepsilon_1)h_1 + (\varepsilon_0/\varepsilon_2)h_2}, \qquad (10)$$

where $\varepsilon_{1,2}$ and $h_{1,2}$ are the dielectric constants and thicknesses of the dielectrics and ε_0 is the permittivity of the intervening gas or liquid. The electrostatic pressure produced by this field is $P_{\rm el} = \varepsilon_0 E^2/8\pi$.

The typical thickness of the deposited layers is $h_{1,2} \sim 100$ nm and the typical concentration of the surface charges is $n_s \sim 10^{12}$ cm^{-2}. Without compensation ($U = 0$), the field in the gap (for the case in which $h_2 = 0$ and $\sigma_2 = 0$) is estimated to be $E = 4\pi\sigma_1/(\varepsilon_1 d + \varepsilon_0 h_1) \sim 10^8$ V/m, where $\varepsilon_1 = 3$ and $\varepsilon_0 = 1$. This field is well above the electrical breakdown of air, $E_b \approx 3 \times 10^6$ V/m, or even of a vacuum, $E_b \sim 10^7$ V/m. This means that there will be an exchange of charges between bodies, tending to reduce the field up to E_b. For example, ions produced in the air gap by the field will be adsorbed on the dielectric surface and screen the trapped charges. Thus, the resulting potential to compensate will be $E_b(\varepsilon_1 d + \varepsilon_0 h)/\varepsilon_1$, and it is estimated to be between one and a few hundred millivolts. It is also interesting to see the effect of the charging on the force. The uncompensated potential results in the electrostatic pressure $P_{\rm el} = \varepsilon_0 E_b^2/8\pi \sim 10^3$ Pa, while the vdW pressure between Si surfaces at $d_0 = 10$ nm is $P_{\rm vdW} = 1.4 \times 10^4$ Pa. Thus, the charges trapped in the dielectric generate the electrostatic force, which is smaller but not negligible compared to the DF.

If metal layers are deposited on Si wafers then the external potential has to compensate the difference between the metal work functions. This difference is typically a few hundred millivolts up to 1 V and it is established by exchange of the carriers. We can carry out the compensation in the same way as for the Casimir force measurements: find a potential that minimizes the total force. In the case of the adhered cantilever the total force will be minimum if the unadhered length is maximum.

IV. CONCLUSIONS

We consider the proposition to measure the dispersion forces (DFs) at short separations using the method of the adhered cantilever. The distances between rough solids close to contact is very inconvenient to measure the forces using the standard method of elastic suspension owing to pull-in instability of the system. However, this distance range (approximately 10 nm) is responsible for many physical phenomena because the DFs are strong enough to compete with the electrostatic forces. The adhered cantilever can be used for measurements in this range of distances because it does not suffer from the instability. We explain the general idea that is based on the sensitivity of the shape of the cantilever to the forces acting near the adhered end. The advantages of the method are no loss of stability at short distances, the force and adhesion energies are measured simultaneously, the force is measured between practically parallel plates, no restrictions on the used materials, and the force in a liquid can be measured with a similar precision as in a gas.

To demonstrate the feasibility of the method, we define the optimal dimensions of the cantilever that guarantee the highest sensitivity to the DFs. We also stress that the method is not applicable for strong adhesion between solids induced by capillary or chemical interactions. We argue that minicantilevers fabricated by micromachining from a piece of single crystalline silicon are able to provide precise measurements. The design of the measuring chip is developed.

The method measures directly the length of the unadhered part of the cantilever s, the maximum deflection from the classic shape of the cantilever $\Delta u_{\rm max}$, and the minimum distance between the solids in contact d_0. All three values can be determined with the precision demanded by a Michelson interferometer with quadrature signals, which provides a necessary wide dynamic range. We conclude that the most important error in the force follows from the uncertainty in d_0.

Finally, we discuss the possibility of reducing the uncertainty in d_0 based on the measured surface roughness and on the contact mechanics that account for the deformation of contacting asperities. This method can be applied only for a rather large adhered area of approximately 1 mm^2, corresponding to the proposed size of the cantilevers. The residual electrostatic interaction is the main background. Although at short separations it is not as severe as at distances $d \sim 100$ nm, it has to be compensated. The most difficult case is realized for dielectrics with trapped charges, but we propose a way to compensate electrostatics, including the case of trapped charges.

ACKNOWLEDGMENTS

This work is supported by the Russian Science Foundation, Grant No. 20-19-00214. G.P. acknowledges support from the Netherlands Organization for Scientific Research (NWO), under Grant No. 16PR3236.

[1] H. B. G. Casimir, On the attraction between two perfectly conducting plates, Proc. Kon. Ned. Akad. Wet. **51**, 793 (1948).
[2] J. Mahanty and B. W. Ninham, *Dispersion Forces (Colloid Science)*, Colloid Science (Academic Press, London, 1976).
[3] E. M. Lifshitz, The theory of molecular attractive forces between solids, Sov. Phys. JETP **2**, 73 (1956).
[4] I. E. Dzyaloshinskii, E. M. Lifshitz, and L. P. Pitaevskii, General theory of van der Waals' forces, Soviet Phys. Usp. **4**, 153 (1961).
[5] G. L. Klimchitskaya, U. Mohideen, and V. M. Mostepanenko, The casimir force between real materials: Experiment and theory, Rev. Mod. Phys. **81**, 1827 (2009).
[6] A. W. Rodriguez, F. Capasso, and S. G. Johnson, The Casimir effect in microstructured geometries, Nat. Photonics **3**, 211 (2011).
[7] S. K. Lamoreaux, Demonstration of the Casimir Force in the 0.6 to 6 μm Range, Phys. Rev. Lett. **78**, 5 (1997).
[8] B. W. Harris, F. Chen, and U. Mohideen, Precision measurement of the casimir force using gold surfaces, Phys. Rev. A **62**, 052109 (2000).
[9] H. B. Chan, V. A. Aksyuk, R. N. Kleiman, D. J. Bishop, and Federico Capasso, Quantum mechanical actuation of microelectromechanical systems by the casimir force, Science **291**, 1941 (2001).
[10] R. S. Decca, D. López, E. Fischbach, and D. E. Krause, Measurement of the Casimir Force between Dissimilar Metals, Phys. Rev. Lett. **91**, 050402 (2003).
[11] R. S. Decca, D. López, E. Fischbach, G. L. Klimchitskaya, D. E. Krause, and V. M. Mostepanenko, Precise comparison of theory and new experiment for the Casimir force leads to stronger constraints on thermal quantum effects and long-range interactions, Ann. Phys. (N. Y.) **318**, 37 (2005).
[12] Davide Iannuzzi, Mariangela Lisanti, and Federico Capasso, Effect of hydrogen-switchable mirrors on the casimir force, Proc. Natl. Acad. Sci. USA **101**, 4019 (2004).
[13] F. Chen, G. L. Klimchitskaya, V. M. Mostepanenko, and U. Mohideen, Demonstration of optically modulated dispersion forces, Opt. Express **15**, 4823 (2007).
[14] S. de Man, K. Heeck, R. J. Wijngaarden, and D. Iannuzzi, Halving the Casimir Force with Conductive Oxides, Phys. Rev. Lett. **103**, 040402 (2009).
[15] G. Torricelli, P. J. van Zwol, O. Shpak, C. Binns, G. Palasantzas, B. J. Kooi, V. B. Svetovoy, and M. Wuttig, Switching casimir forces with phase-change materials, Phys. Rev. A **82**, 010101 (2010).
[16] Gauthier Torricelli, Peter J. van Zwol, Olex Shpak, George Palasantzas, Vitaly B. Svetovoy, Chris Binns, Bart J. Kooi, Peter Jost, and Matthias Wuttig, Casimir force contrast between amorphous and crystalline phases of aist, Adv. Funct. Mater. **22**, 3729 (2012).
[17] Niels Tas, Tonny Sonnenberg, Henri Jansen, Rob Legtenberg, and Miko Elwenspoek, Stiction in surface micromachining, J. Micromech. Microeng. **6**, 385 (1996).
[18] Roya Maboudian and Roger T. Howe, Critical review: Adhesion in surface micromechanical structures, J. Vacuum Sci. Technol. B **15**, 1 (1997).
[19] E. E. Parker, W. R. Ashurst, C. Carraro, and R. Maboudian, Adhesion characteristics of mems in microfluidic environments, J. Microelectromech. Syst. **14**, 947 (2005).
[20] Kellar Autumn, Metin Sitti, Yiching A. Liang, Anne M. Peattie, Wendy R. Hansen, Simon Sponberg, Thomas W. Kenny, Ronald Fearing, Jacob N. Israelachvili, and Robert J. Full, Evidence for van der Waals adhesion in gecko setae, Proc. Natl. Acad. Sci. USA **99**, 12252 (2002).
[21] Bharat Bhushan, Adhesion and stiction: Mechanisms, measurement techniques, and methods for reduction, J. Vac. Sci. Technol. B **21**, 2262 (2003).
[22] Philip Ball, Feel the force, Nature **447**, 772 (2007).
[23] F. Capasso, J. N. Munday, D. Iannuzzi, and H. B. Chan, Casimir forces and quantum electrodynamical torques: Physics and nanomechanics, IEEE J. Sel. Top. Quant. **13**, 400 (2007).
[24] E. Buks and M. L. Roukes, Stiction, adhesion energy, and the casimir effect in micromechanical systems, Phys. Rev. B **63**, 033402 (2001).
[25] G. Palasantzas and J. Th. M. DeHosson, Phase maps of microelectromechanical switches in the presence of electrostatic and casimir forces, Phys. Rev. B **72**, 121409 (2005).
[26] G. Palasantzas and J. Th. M. De Hosson, Pull-in characteristics of electromechanical switches in the presence of casimir forces: Influence of self-affine surface roughness, Phys. Rev. B **72**, 115426 (2005).
[27] F. W. DelRio, M. P. de Boer, J. A. Knapp, E. D. Reedy, P. J. Clews, and M. L. Dunn, The role of van der waals forces in adhesion of micromachined surfaces, Nat. Mater. **4**, 629 (2005).
[28] R. Esquivel-Sirvent, L. Reyes, and J. Bárcenas, Stability and the proximity theorem in casimir actuated nano devices, New J. Phys. **8**, 241 (2006).
[29] R. Esquivel-Sirvent, M. A. Palomino-Ovando, and G. H. Cocoletzi, Pull-in control due to casimir forces using external magnetic fields, Appl. Phys. Lett. **95**, 051909 (2009).
[30] Wijnand Broer, George Palasantzas, Jasper Knoester, and Vitaly B. Svetovoy, Significance of the casimir force and

surface roughness for actuation dynamics of mems, Phys. Rev. B **87**, 125413 (2013).

[31] Wijnand Broer, Holger Waalkens, Vitaly B. Svetovoy, Jasper Knoester, and George Palasantzas, Nonlinear Actuation Dynamics of Driven Casimir Oscillators with Rough Surfaces, Phys. Rev. Appl. **4**, 054016 (2015).

[32] M. Sedighi, W. H. Broer, S. Van der Veeke, V. B. Svetovoy, and G. Palasantzas, Influence of materials optical response on actuation dynamics by Casimir forces, J. Phys. – Condens. Mat. **27**, 214014 (2015).

[33] G. Bressi, G. Carugno, R. Onofrio, and G. Ruoso, Measurement of the Casimir Force between Parallel Metallic Surfaces, Phys. Rev. Lett. **88**, 041804 (2002).

[34] P. J. van Zwol, G. Palasantzas, M. van de Schootbrugge, and J. Th. M. De Hosson, Measurement of dispersive forces between evaporated metal surfaces in the range below 100nm, Appl. Phys. Lett. **92**, 054101 (2008).

[35] J. Israelachvili, Y. Min, M. Akbulut, A. Alig, G. Carver, W. Greene, K. Kristiansen, E. Meyer, N. Pesika, K. Rosenberg, and H. Zeng, Recent advances in the surface forces apparatus (SFA) technique, Rep. Prog. Phys. **73**, 036601 (2010).

[36] A. Tonck, F. Houze, L. Boyer, J. L. Loubet, and J. M. Georges, Electrical and mechanical contact between rough gold surfaces in air, J. Phys. Condens. Matter **3**, 5195 (1991).

[37] M. Sedighi, V. B. Svetovoy, and G. Palasantzas, Casimir force measurements from silicon carbide surfaces, Phys. Rev. B **93**, 085434 (2016).

[38] C. Genet, A. Lambrecht, P. Maia Neto, and S. Reynaud, The Casimir force between rough metallic plates, Europhys. Lett. **62**, 484 (2003).

[39] Paulo A. Maia Neto, Astrid Lambrecht, and Serge Reynaud, Casimir effect with rough metallic mirrors, Phys. Rev. A **72**, 012115 (2005).

[40] V. B. Svetovoy and G. Palasantzas, Influence of surface roughness on dispersion forces, Adv. Colloid Interface Sci. **216**, 1 (2015).

[41] P. J. van Zwol, G. Palasantzas, and J. Th. M. De Hosson, Influence of random roughness on the casimir force at small separations, Phys. Rev. B **77**, 075412 (2008).

[42] Wijnand Broer, George Palasantzas, Jasper Knoester, and Vitaly B. Svetovoy, Roughness correction to the Casimir force beyond perturbation theory, EPL (Europhys. Lett.) **95**, 30001 (2011).

[43] Wijnand Broer, George Palasantzas, Jasper Knoester, and Vitaly B. Svetovoy, Roughness correction to the Casimir force at short separations: Contact distance and extreme value statistics, Phys. Rev. B **85**, 155410 (2012).

[44] P. J. van Zwol, V. B. Svetovoy, and G. Palasantzas, Distance upon contact: Determination from roughness profile, Phys. Rev. B **80**, 235401 (2009).

[45] C. H. Mastrangelo and C. H. Hsu, Mechanical stability and adhesion of microstructures under capillary forces. I. Basic theory, J. Microelectromech. Syst. **2**, 33 (1993).

[46] C. H. Mastrangelo and C. H. Hsu, Mechanical stability and adhesion of microstructures under capillary forces. II. Experiments, J. Microelectromech. Syst. **2**, 44 (1993).

[47] M. P. de Boer and T. A. Michalske, Accurate method for determining adhesion of cantilever beams, J. Appl. Phys. **86**, 817 (1999).

[48] J. A. Knapp and M. P. de Boer, Mechanics of microcantilever beams subject to combined electrostatic and adhesive forces, J. Microelectromech. Syst. **11**, 754 (2002).

[49] V. B. Svetovoy, A. E. Melenev, M. V. Lokhanin, and G. Palasantzas, Global consequences of a local Casimir force: Adhered cantilever, Appl. Phys. Lett. **111**, 011603 (2017).

[50] G. Palasantzas, V. B. Svetovoy, and P. J. van Zwol, Optical properties and kinetic roughening influence on dispersive Casimir and van der Waals forces, Int. J. Mod. Phys. B **24**, 6013 (2010).

[51] B. D. Jensen, M. P. de Boer, N. D. Masters, F. Bitsie, and D. A. LaVan, Interferometry of actuated microcantilevers to determine material properties and test structure nonidealities in mems, J. Microelectromech. Syst. **10**, 336 (2001).

[52] R. Reibold and W. Molkenstruck, Laser interferometric measurement and computerized evaluation of ultrasonic displacements, Acta Acustica **49**, 207 (1981).

[53] T. Požar and J. Možina, Enhanced ellipse fitting in a two-detector homodyne quadrature laser interferometer, Meas. Sci. Technol. **22**, 085301 (2011).

[54] Ilia V. Uvarov, Mikhail V. Lokhanin, Alexander V. Postnikov, Artem E. Melenev, and Vitaly B. Svetovoy, Electrochemical membrane microactuator with a millisecond response time, Sens., Actuator. B-Chem. **260**, 12 (2018).

[55] V. A. Parsegian, *Van der Waals Forces* (Cambridge University Press, New York, 2006).

[56] G. L. Klimchitskaya, U. Mohideen, and V. M. Mostepanenko, Casimir and van der Waals forces between two plates or a sphere (lens) above a plate made of real metals, Phys. Rev. A **61**, 062107 (2000).